2016

Theoretical and Experimental Investigation on Dewatering Performance from Aqueous Lithium Bromide Solution Stream confined by Hollow Fiber Membrane

Sung Joo Hong
University of Tokyo, Japan, gatorhong@gmail.com

Eiji Hihara
University of Tokyo, Japan, hihara@k.u-tokyo.ac.jp

Chaobin Dang
University of Tokyo, Japan, dangcb@k.u-tokyo.ac.jp

Theoretical and experimental investigation on dewatering performance from aqueous lithium bromide solution stream confined by hollow fiber membrane

Sung Joo HONG, Eiji HIHARA, Chaobin DANG*

Department of Human and Engineered Environmental studies, Graduate School of Frontier Science, The University of Tokyo, 5-1-5 Kashiwanoha, Kashiwa-shi, Chiba 277-8563, Japan
Email: dangcb@k.u-tokyo.ac.jp, TEL/FAX: +81 4 7136 4647

ABSTRACT

Vapor absorption refrigeration system efficiently could be driven by the low grade renewable heat associated with the exhaust gas from the car engine, and uses the eco-friendly refrigerant, i.e. water. The absorption cycle, however, has not yet obtained much attraction in the automobile application due to its large volume and weight per unit of cooling capacity, which has limited to use. A micro-porous hydrophobic membrane acts as a selective barrier which allows water vapor to pass through but blocks the passage of liquid solution, and therefore as an application of VARs, it is expected that a hydrophobic hollow fiber membrane module is introduced for a generator by extracting the refrigerant vapor from the liquid LiBr solution stream which is mechanically constrained by the hydrophobic layers. In this study a hollow fiber membrane-based generator is introduced, and theoretically and experimentally investigated. The mass transfer performance through membranes is analyzed under various operating conditions.

1. INTRODUCTION

In general, automobile manufacturers employ vapor compression refrigeration system (VCRs) for car air-conditioning system owing to their small size and high performance-to-volume ratio, but they have two major drawbacks: the large energy consumption by a compressor, and the use of hydrocarbon derivatives causing environmental problems. On the other hand, vapor absorption refrigeration system (VARs) has several benefits over VCRs: the use of an eco-friendly refrigerant and low-grade heat source to operate the system. Therefore, there is increasing interest in the use of VARs in automobiles although the system needs to be sufficiently scaled down and its weight needs to be reduced while maintaining its high performance. In the conventional generator in VARs, the free surface of aqueous solution exists in the region where the evaporation occurs, making the system performance unstable when a vehicle drives on hills, or undergoes unexpected vibrations [1].

A micro-porous hydrophobic membrane is defined as a selective barrier that enables a certain component to pass through but blocks the passage of others. In general, a hollow fiber membrane (HFM) module has been mainly utilized in various industrial fields, related to waste water treatments, desalination, water purification, food industry [2-5]. As an application of VARs, it is expected that the HFM module acts as a generator by extracting the refrigerant i.e. water vapor from a stream of aqueous LiBr solution constrained mechanically by the hydrophobic HFM layers [6]. The constrained flow of LiBr solution prevents the performance degradation associated with vibrations and slopes while driving from affecting the VARs. Further, the HFM-based module is smaller and lighter than the conventional generator in VARs. An automobile engine can provide a relatively high temperature heat source [7]. Based on this point of view, we present a HFM-based generator (HFM-G) in this paper. In order to clarify the permeability of water vapor across the membrane, the theoretical and experimental works were conducted on the membrane distillation performance of a HFM module.

2. THEORY

Figure 1 presents a schematic of (a) the HFM-G used in experiments and (b) the principle of water vapor evaporation from the liquid LiBr solution stream confined by a micro-porous hydrophobic HFM. This aqueous solution cannot permeate into the hydrophobic membrane pores due to large capillary action; however, it can penetrate the

pores if the pressure difference across the membrane exceeds a certain value called the liquid entry pressure (LEP) [8]:

$$LEP = -\frac{2\sigma\cos\theta}{r_p} \tag{1}$$

where σ, θ, and r_p are the surface tension of the liquid, the contact angle between the liquid and membrane surface, and pore radius, respectively.

Water vapor evaporates from the liquid/vapor interface (see the curvature liquid/vapor interface in Fig.1b), and passes through the membrane pores so long as the permeate side is maintained at a pressure below the equilibrium vapor pressure of the feed [9]. During the evaporation process, there is a large temperature drop between the inlet and outlet of the HFM-G, associated with the latent heat of vaporization. As liquid LiBr solution flows along the length of the HFM-G and as refrigerant vapor escapes from the solution flow, the mass flux of the vapor penetrating through the membrane decreases because of the change in partial pressure of refrigerant vapor due to the decrease in temperature and the increase in concentration.

2.1 Mass transfer mechanism

The mass flux of water vapor penetrating the pores is proportional to the partial vapor pressure difference across the membrane. According to Darcy's law, the mass flux is determined by the membrane distillation coefficient, B_m [10]:

$$J_v = B_m(p_{p,m,s} - p_{p,p}) \tag{2}$$

where $P_{p,m,s}$ is the partial pressure of the refrigerant vapor at the membrane surface, and $P_{p,p}$ is the pressure at the permeate side, i.e. condenser pressure in this study. The dominant transport mechanism is assumed to be the Knudsen diffusion with submicron pores and low pressure at the shell side, where the membrane distillation coefficient B_m, is expressed as [11] follows:

$$B_m = 1.064\frac{r_p\phi}{\delta\tau}\left(\frac{M}{RT_m}\right)^{0.5} \tag{3}$$

where Φ, τ, and δ are membrane porosity, membrane tortuosity, and membrane thickness, respectively; M, R, and T_m are the molecular weight of vapor, gas constant, and temperature of membrane pores, respectively.

The mass flux across the membrane depends on the partial pressure of water vapor, which is a function of the temperature and concentration at the liquid/vapor interface. Thin film theory can be applied to determine the concentration profile at the membrane surface [12]:

$$c_{m,s} = c_{b,f}\exp\left(\frac{J_v}{\rho\alpha}\right) \tag{4}$$

where ρ and α are the density and convective mass transfer coefficient, respectively.

2.1 Heat transfer mechanism

Since pressure of the permeate side is maintained identical to the condensation pressure, which is very low, the model represents vacuum membrane distillation (VMD). In VMD, heat and mass transfer through the membrane occur simultaneously (*Fig.3*). Convective heat transfer across the feed thermal boundary layer developed adjacent to the membrane surface occurs from the bulk phase to the solution/membrane interface:

$$\Delta Q_f = h_f(T_b - T_{m,s})\pi d_{in}\Delta x \tag{5}$$

where ΔQ_f is the heat transfer by the convection, and h_f is the convective heat transfer coefficient. T_b and $T_{m,s}$ are the bulk temperature of the solution and the membrane surface temperature, respectively. d_{in} is the inner diameter of the membrane, and Δx is the interval in the flow direction.

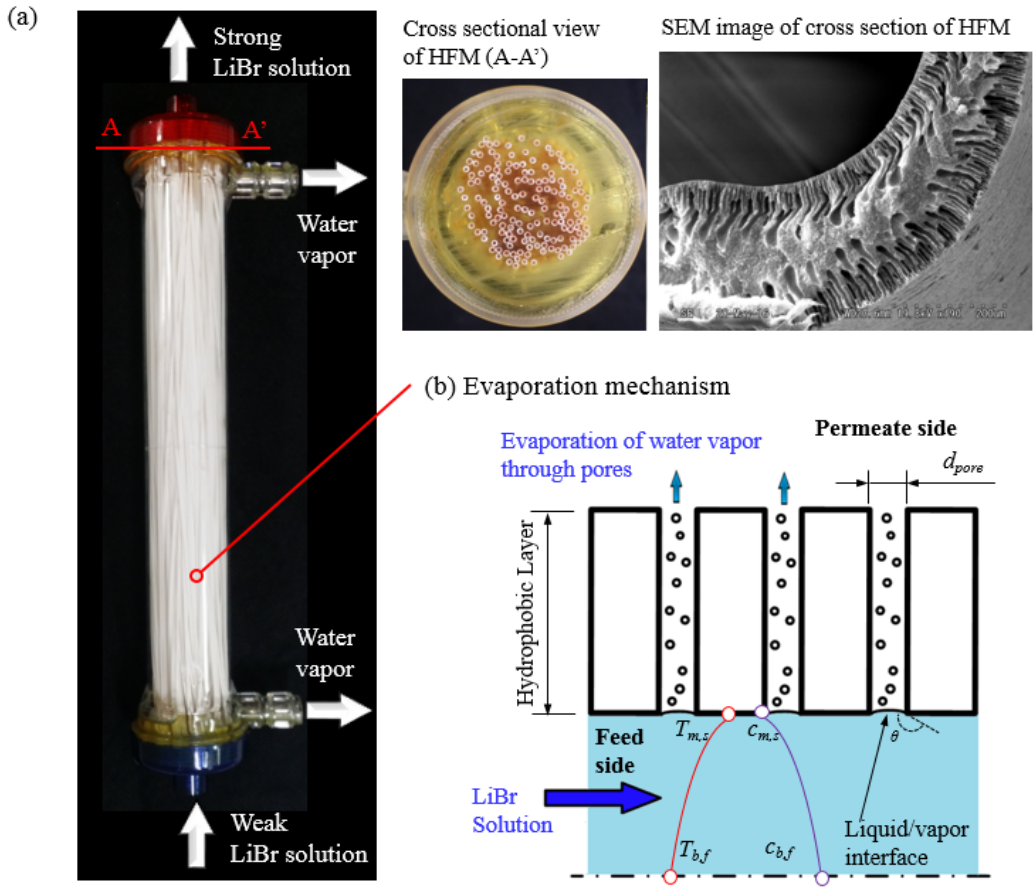

Fig. 1. (a) HFM-G used in experiments, (b) principle of water vapor evaporation from the liquid LiBr solution stream confined by a micro-porous hydrophobic HFM

The heat transfer rate by vapor flux across the membrane is as follows:

$$\Delta Q_m = J_v H_v \pi d_{in} \Delta x \tag{6}$$

where H_v is the heat of vaporization of water.

Consequently, in a steady state, the total energy balance is expressed by the following relation.

$$\Delta Q_f = \Delta Q_m \tag{7}$$

Here, the conventional empirical correlations for the convective heat transfer coefficient h_f may not be valid because the membrane is a porous and non-rigid body. In such a case, the convective heat transfer coefficient for laminar flow is evaluated by using the Leveque equation as shown below [13]:

$$Nu = \frac{h_f d_i}{k} = 1.86 \left(\frac{Re\, Pr\, d_i}{L} \right)^{0.33} \tag{8}$$

where Nu, d_i, and k are the Nusselt number, the inner diameter of the membrane, and the thermal conductivity of fluid, respectively. Re is Reynolds number, and Pr is Prandtl number. L is the length of the membrane.

3. EXPERIMENTAL

3.1 Experimental setup

Fig.2a presents a schematic diagram of experimental apparatus to measure the desorption performance of water vapor from aqueous LiBr solution stream through the HFM-G under static vacuum pressure. Feed weak LiBr solution circulated by a solution pump passes through an inlet Coriolis flow meter to measure the density, temperature and flow rate of weak solution. The LiBr solution heated up by a heat exchanger enters the HFM-G, and the evaporation process takes place so that water vapor comes into a condenser. Pressure of the permeate side is controlled and kept by cooling process in the condenser. Strong LiBr solution which leaves the HFM-G flows into an outlet Coriolis flow meter also to measure the density and temperature of the strong solution. The strong solution enters a LiBr solution tank, and is recirculated. The membrane parameters and the operating conditions for experiments are presented in Table. 1.

3.2 Experimental methodology

All the experimental data is obtained under steady state condition. Two Coriolis flow meters (accuracy ±0.0005g/mL in density, ALTI mass CA003, OVAL) collect the density of both the weak and strong LiBr solution, and each solution temperatures are also measured by thermocouples. Both the concentrations of weak and strong solution are calculated by the density and temperature data to evaluate the mass transport of water vapor [14]. As shown in *Fig.2b*, the concentration of the weak solution keeps increasing during the experiments as the water vapor escapes from the HFM-G. Thus, the mass flux performance is investigated with respect to each concentration of feed LiBr solution. Both the inlet and outlet solution temperatures are measured by two resistance thermometer (PT100 class A, Chino) to obtain the temperature drop by the evaporation process. Vacuum pressure at condenser was measured by a ceramic capacitance manometer (accuracy 0.2%, CCMT-100D, ULVAC).

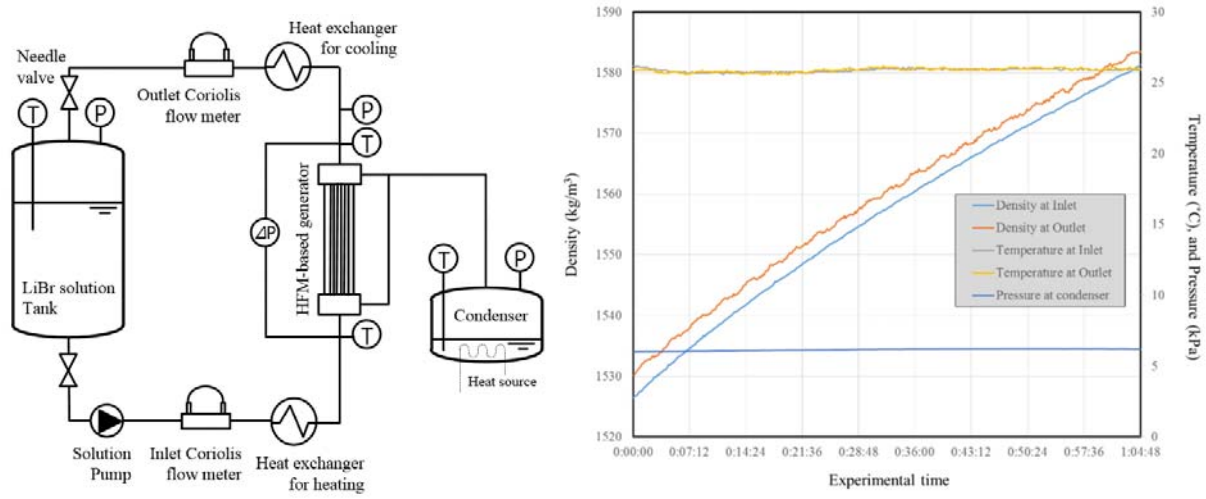

Fig.2. (a) Schematic of experimental apparatus, (b) Experimental methodology

Table 1: Membrane parameters and experimental operating conditions

Parameters	Values
Number of hollow fiber membrane	100
Material of hollow fiber membrane	PVDF
Pore diameter of hollow fiber membrane [μm]	0.16
Inner diameter of hollow fiber membrane [μm]	800
Outer diameter of hollow fiber membrane [μm]	1100
Length of hollow fiber membrane [cm]	30
Temperature of feed solution [°C]	55 - 74
Velocity of feed solution in the hollow fiber membrane [cm/s]	9.1 – 13.2
Pressure at permeate side [kPa]	3.4, 5.3
Concentration range of feed solution (%)	51 - 59

4. RESULTS AND DISCUSSION

4.1 Theoretical study

4.1.1 Effect of feed solution temperature and flow rate on mass transport

As shown in *Fig. 3a*, the generating temperature directly influences the concentration difference between the inlet and outlet of the HFM-G at constant vacuum pressure. The concentration difference, however, decreases with an increase in mass flow rate of feed solution, i.e. velocity of solution, because the membrane distillation efficiency, defined as the ratio of the evaporated refrigerant vapor to the energy input decreases under the certain membrane parameters. At higher generating temperature, the solution concentration at the outlet of HFM-G becomes exponentially stronger because the membrane distillation performance depends strongly on the feed temperature. Thus, to practically use the HFM-G for VARs, the circulation ratio, defined as the ratio of flow rate of feed solution to refrigerant, becomes extremely reduced at a higher feed solution temperature. The circulation ratio is a significant design and optimizing factor as it directly influences the size and cost of the generator. *Fig. 3b* describes the mass flux of refrigerant vapor extracted from the HFM-G with respect to both the mass flow rate and temperature of feed solution. As the mass flow rate of solution increases, the rate of temperature drop (i.e. driving force of mass transport) in the flowing direction decreases. Therefore the increase in both the feed flow rate and temperature of solution significantly lead to the higher mass flux of the refrigerant vapor.

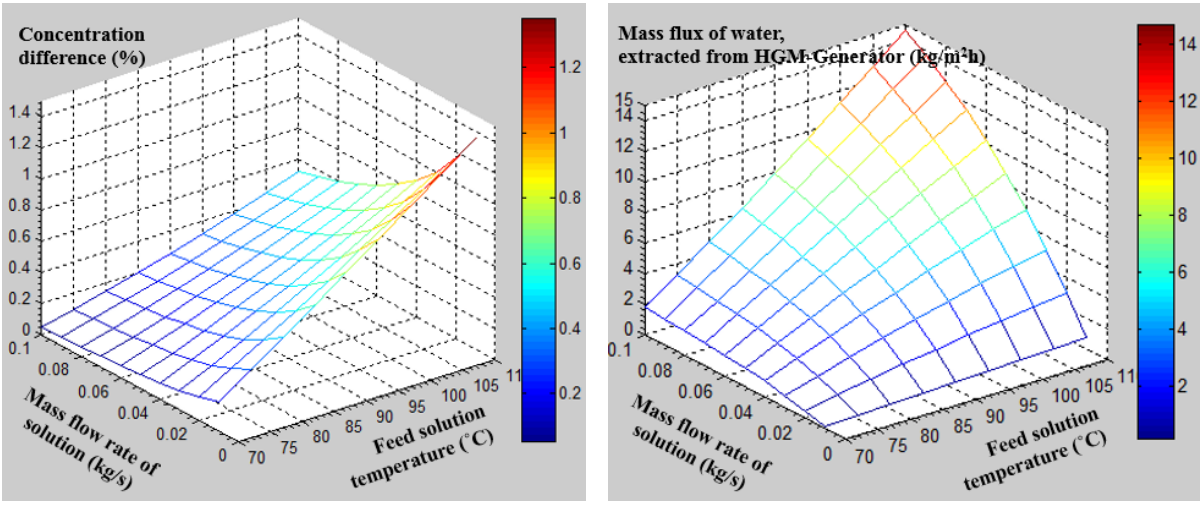

Fig. 3. (a) Concentration difference between inlet and outlet of HFM-G with respect to feed solution temperature and mass flow rate of solution (x_{inlet} = 50%, $P_{permeate}$ = 7 kPa), (b) Mass flux of refrigerant vapor with respect to feed solution temperature and mass flow rate of solution (T_{feed} = 100℃, x_{inlet} = 50%, $P_{permeate}$ = 7 kPa)

4.1.2 Effect of the number and length of HFMs on mass transport

Fig. 4a and 4b present the simulation results on the mass transfer performance with respect to the number and length of HFMs. The HFM-G has a great advantage that the number of HFMs is easily adjusted for a given volume of the module so that the contact area for evaporation of refrigerant vapor increases to control its performance. The increases in both the number and length of HFMs enhance the concentration difference. The *Fig. 4a*, however, shows the curve for the concentration difference becomes almost flat and hardly varies as the independent variables of HFM increase. The change in the number of HFMs is associated with the solution velocity and the change in length of HFMs is related with the decrease in the driving force in the flowing direction. That is, the driving force of mass transport drastically decreases as the solution temperature decreases, and thus the mass transfer across the membrane layers is hardly occurred in the flow direction. The mass flux of refrigerant vapor decreases with the increases in both the number and length of HMFs, as shown in *Fig. 4b*. Note that the sensible heat at the inlet of the HFM-G provides the energy for evaporation. Thus, regardless of the number and length of HFMs, the improvement in the distillation performance is limited because the performance depends completely on the given feed solution conditions.

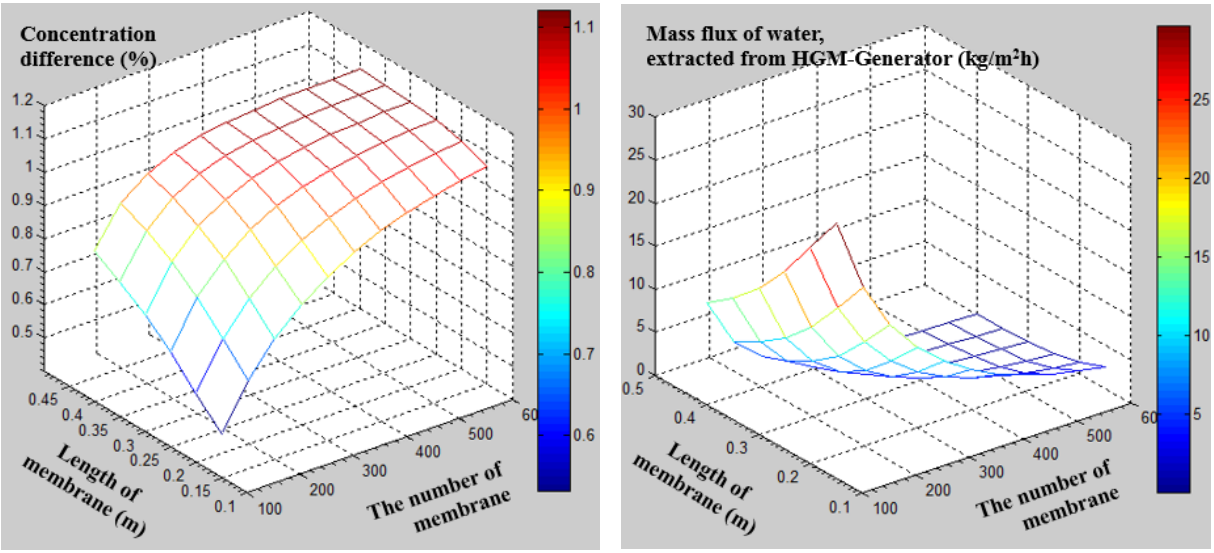

Fig. 4. (a) Concentration difference between inlet and outlet of HFM-G with respect to the number and length of HFM (T_{feed} = 100℃, x_{inlet} = 50%, $P_{permeate}$ = 7 kPa), (b) Mass flux of refrigerant vapor with respect to the number and length of HFM (T_{feed} = 100℃, x_{inlet} = 50%, $P_{permeate}$ = 7 kPa)

4.2 Experimental study

4.2.1 Effects of feed solution velocity on mass flux of water vapor

Fig.5a presents the experimental data on the concentration difference between the inlet and outlet of HFM-G as a function of temperature of the feed solution with three different solution concentration. The lower concentration of the feed solution has more potential to evaporate the refrigerant vapor, and thus more evaporation takes place when lower concentration of solution is fed into HFM-G. The fitted curves indicate the exponential increases, leading to the fact that the feed temperature has a significant factor to enhance the mass flux of refrigerant vapor.

4.2.2 Effects of feed solution velocity on mass flux of water vapor

Mass transfer performance is experimentally investigated with respect to the feed solution velocity, as shown in *Fig. 5b*. It is shown that the mass flux of refrigerant vapor increases with the feed solution velocity because the higher sensible energy input is used for more evaporation of refrigerant as aforementioned in the theoretical approach.

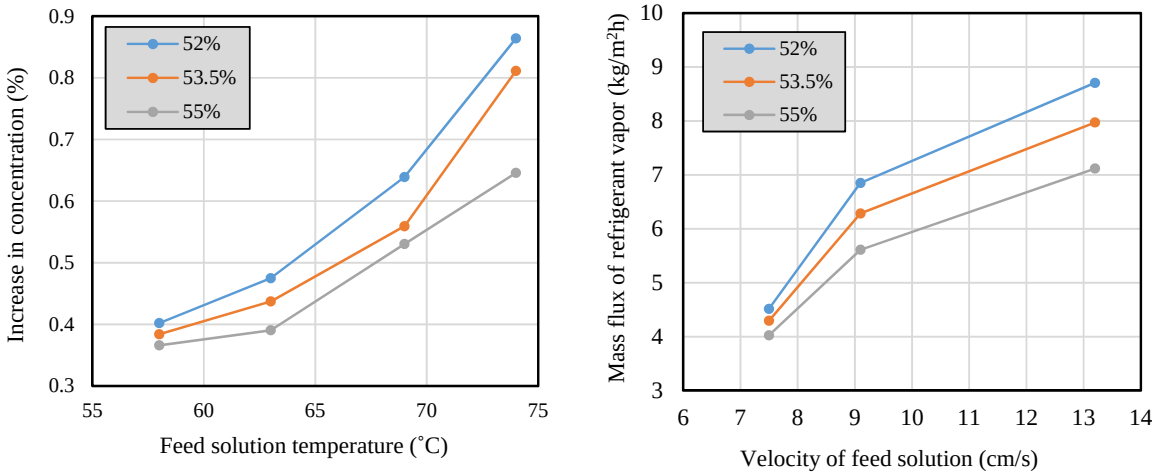

Fig. 5. (a) Concentration difference between inlet and outlet of HFM-G with respect to feed solution temperature

with three different solution concentration (u_{feed} = 9.1 cm/s, $P_{permeate}$ = 5.3 kPa), (b) Mass flux of refrigerant vapor with respect to solution velocity with three different solution concentration (T_{feed} = 74 ℃, $P_{permeate}$ = 3.4 kPa)

4.5 Comparison of theoretical model with experimental data

Fig.6 describes the comparison results of theoretical values with experimental data. During each experiment, the concentration of feed solution decreases as the refrigerant vapor is extracted. The mass flux decreases as the feed concentration increases due to less evaporation potential, i.e. less water vapor is contained in the solution. As the feed temperature and velocity of solution increase, the mass flux also increases. The results show that the theoretical model could predict the mass flux performance with error of less than 20% at relatively higher temperature and velocity of feed solution. However, at the lower feed temperature and the lower solution velocity, the error becomes larger.

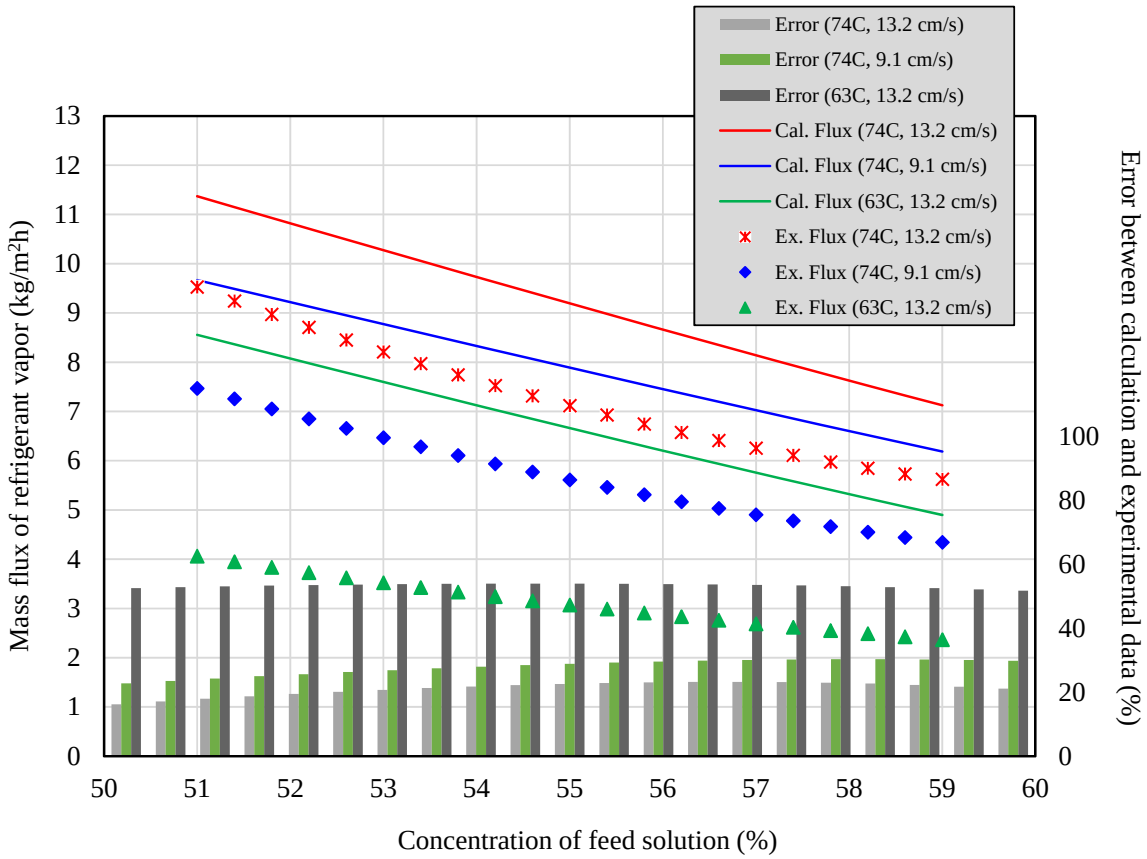

Fig. 6. Mass flux of refrigerant vapor with respect to concentration of feed solution for several operating conditions (T_{feed} = 63, 74℃, u_{feed} = 9.1, 13.2 cm/s, $P_{permeate}$ = 3.4 kPa)

5. CONCLUSION

In this study, a hollow fiber membrane-based generator for vapor absorption refrigeration system was proposed for application in automobiles. Theoretical approach and experimental works are presented to investigate the mass transfer performance of refrigerant vapor emerged from HFM-G. Main conclusion can be drawn as follows:

- A higher generating temperature is essential for enhancing the mass transfer performance, and for reducing the system scale
- Since the number of HFMs could be easily adjusted for a given volume of the module, the system is scaled down and made lighter. The length of HMFs is also adjusted to control the mass transfer performance.

- Theoretical simulation data was compared with experimental data. At relatively higher temperature and velocity of feed solution, the theoretical model predicted the mass flux performance with error of less than 20%. The error, however, became larger at lower temperature and velocity of feed solution.

The HFM-G has enormous potential to replace the conventional generator in VARS. The membrane distillation performance could be improved by varying the membrane parameters, such as pore size, thickness, and inner diameter of the membrane. For the further research, the theoretical optimization work is necessary for the practical use.

REFERENCES

[1] J. Koehler, W. J. Tegethoff, D. Westphalen, M. Sonnekalb, "Absorption refrigeration system for mobile applications utilizing exhaust gases", Heat and Mass Transfer 32 (1997) 333-340
[2] Y. Shimizu, Y. I. Okuno, K. Uryu, S. Ohtsubo, A. Watanabe, "Filtration characteristics of hollow fiber microfiltration membranes used in membrane bioreactor for domestic wastewater treatment", Water Research (1996) Vol. 30, No. 10, pp. 2385-239
[3] C. Cabassud, D. Wirth, "Membrane distillation for water desalination: how to chose an appropriate membrane?", Desalination 157 (2003) 307-314
[4] A. M. Urtiaga, E. D. Gorri, G. Ruiz, I. Ortiz, "Parallelism and differences of pervaporation and vacuum membrane distillation in the removal of VOCs from aqueous streams", Separation and Purification Technology 22-23 (2001) 327–337
[5] S. Nene, S. Kaur, K. Sumod, B. Joshi, K.S.M.S. Raghavarao" "Membrane distillation for the concentration of raw cane-sugar syrup and membrane clarified sugarcane juice", Desalination 147 (2002) 157-160
[6] S. J. Hong, E. Hihara, C. Dang, "Novel absorption refrigeration system with a hollow fiber membrane-based generator", International Journal of Refrigeration (2016)
[7] H. L. Talom, A. Beyene, "Heat recovery from automotive engine", Applied Thermal Engineering 29 (2009) 439-444
[8] A. C. M. Franken, J. A. M. Nolten, M. H. V. Mulder, D. Bargeman, C. A. Smolders, "Wetting criteria for the applicability of membrane distillation", Journal of Membrane Science 33 (3) (1987) 315-328
[9] S. Bandini, A. Saavedra, G. C. Sarti, "Vacuum Membrane Distillation: Experiments and Modeling", AlchE Journal 43 (2) (1997)
[10] L. Pena, M. P. Godino, J. I. Mengual, "A method to evaluate the net membrane distillation coefficient", Journal of Membrane Science 143 (1998) 219-233
[11] J. G. Lee, W.-S. Kim, "Numerical modeling of the vacuum membrane distillation process", Desalination 331 (2013) 46-55
[12] V. A. Bui, L. T. T. Vub, M. H. Nguyen, "Modelling the simultaneous heat and mass transfer of direct contact membrane distillation in hollow fibre modules", Journal of Membrane Science, 353, Issues 1–2 (2010) 85-93
[13] B. Li, K. K. Sirkar, "Novel membrane and device for vacuum membrane distillation-based desalination process", Journal of Membrane Science 257 (2005) 60-75
[14] M.R.Patterson, "Numerical fits of the properties of lithium-bromide water solutions", ASHRAE (1988) Transactions 94(2)

ACKNOWLEDGEMENT

This paper is based on results obtained from a project commissioned by the New Energy and Industrial Technology Development Organization (NEDO).